



Biomechanical simulation of forces and moments of initial orthodontic tooth movement in dependence on the used archwire system by ROSS (Robot Orthodontic Measurement & Simulation System)

Benedikt Dotzer^a, Thomas Stocker^a, Andrea Wichelhaus^a, Mila Janjic Rankovic^a, Hisham Sabbagh^{a,*}

^a Department of Orthodontics and Dentofacial Orthopedics, University Hospital, LMU Munich, Goethestrasse 70, Munich 80336, Germany



ARTICLE INFO

Keywords:

Biomechanics
Robotics
Orthodontic simulation
Orthodontic tooth movement
Force control
Leveling archwire

ABSTRACT

Objectives: Aim of this study was to determine the forces and moments during simulated initial orthodontic tooth movements using a novel biomechanical test setup.

Methods: The test setup consisted of an industrial precision robot with a force-torque sensor, a maxillary model and a control computer and software. Forces and moments acting on the corresponding experimental tooth during the motion simulations were dynamically measured for two 0.016" NiTi round archwires (Sentalloy Light/Sentalloy Medium). Intrusive (#1), rotational (#2) and angular (#3) tooth movements were simulated by a control program based on the principle of force control and executed by the robot. The results were statistically analysed using K-S-test and Mann-Whitney *U* test with a significance level of $\alpha = 5\%$.

Results: Sentalloy Medium archwires generated higher forces and moments than the Sentalloy Light archwires in all simulations. In simulation #1 the mean initial forces/moment reached 1.442 N/6.781 Nmm for the Light archwires and 1.637 N/9.609 Nmm for the Medium archwires. In movement #2 Light archwires generated mean initial forces/moment of 0.302 N/-8.271 Nmm whereas Medium archwires generated 0.432 N/-9.653 Nmm. Simulation #3 showed mean initial forces/moment of -0.122 N/8.477 Nmm from the Light archwires compared to -0.300 N/11.486 Nmm for the Medium archwires.

Significance: The measured forces and moments were suitable for initial orthodontic tooth movement in simulations #2 and #3, however inadequate in simulation #1. Reduced archwire dimensions ($<0.016"$) should be selected for initial leveling of vertical malocclusions.

1. Introduction

Orthodontic multibracket appliances are widely used for the treatment of malocclusions (Graber et al., 2022; Proffit et al., 2007). In these systems, archwires can be used to apply forces and moments to the teeth to induce tooth movements (Burstone and Koenig, 1974). Orthodontic tooth movement is achieved by a biological reaction in terms of bone remodeling, as a result of a complex interaction between the cells of the periodontal ligament, the bone matrix, hormones, cytokines, and growth factors (Xu et al., 2022; Zhang et al., 2022; Jeon et al., 2021). For a clinically efficient tooth movement with minimal hyalinization and pain, as well as a reduced risk of apical root resorption (ARR), the application of suitable force and moment magnitudes is required (Reitan, 1957, 1960, 1967, 1985; Wichelhaus, 2013; Wichelhaus et al.,

2021).

However, in clinical practice, it is often difficult for the practitioner to accurately estimate the magnitude and direction of the forces and moments that will develop within an orthodontic appliance (Koenig et al., 1980). Since intraoral measurements are limited, in-vitro studies have been conducted in the field of biomechanics to investigate orthodontic appliances, mostly applying biomechanical test stands or finite element (FE) simulations (Friedrich et al., 1999; Mascarenhas et al., 2018; Rajgopal, 2022; Adel et al., 2021).

Numerical methods such as the finite element method (FEM) are increasingly being applied due to advances in computer technology, as they allow the simulation of complex and adaptive models of biological systems and processes (Cicciu, 2020; Cervino et al., 2020; Singh et al., 2016; Ahuja et al., 2018; de Brito et al., 2019). These digital simulations

* Corresponding author.

E-mail address: hisham.sabbagh@med.uni-muenchen.de (H. Sabbagh).

are usually performed based on experimentally determined parameters, but also on simplified assumptions (Hayashi et al., 2007; Romanyk et al., 2020; Wanju et al., 2015; Ammar et al., 2011). Biomechanical test stands, on the other hand, are less adaptable than computer models, but allow the investigation of the actual underlying physical properties of materials, specimens and appliances without the influence of subjectively determined parameters. One difficulty, however, is the biomechanical simulation of dynamic processes as they occur during orthodontic treatment, since the resulting force-moment systems are constantly changing due to the continuous tooth movements. To overcome these limitations, more complex, computerized and robotic biomechanical test stands have been developed. (Bourauel et al., 1992; Fuck and Drescher, 2006; Fansa et al., 2009; Pandis et al., 2009; Badawi et al., 2009; Chen et al., 2007, 2010). In 1992, the "OMSS – Orthodontic Measurement and Simulation System" was introduced to conduct computer-assisted examinations of tooth movements in relation to the forces and moments acting on them (Bourauel et al., 1992). In 2006 the "Robotic Measurement System" (RMS) was introduced, using a robot in the experimental setup to investigate the initial force systems generated by different leveling archwires (Fuck and Drescher, 2006). However, due to the static experimental setup, it was not possible to track the dynamic changes of the archwire forces and moments. By programming feedback between measured force-moment values and movements executed automatically by robots, dynamic motion sequences can be simulated. The conduct of such biomechanical investigations is complex, thus only few test stands have been validated and employed to date (Badawi et al., 2009; Liu et al., 2014).

Aim of this study is to determine the forces and moments of a fixed multibracket appliance dynamically during simulated initial tooth movements using a novel biomechanical test setup.

2. Materials and methods

2.1. Development of the test stand

The test setup used was developed in the Biomechanics Laboratory of the Department of Orthodontics and Dentofacial Orthopedics of the LMU University Hospital. The core component of the setup was an industrial precision robot KUKA KR 5-sixx R650 (KUKA Roboter GmbH, Germany) with six degrees of freedom. At the top of the robot, a FTS Nano 17 SI-12-0.12 force-torque sensor (ATI Industrial Automation, USA), which can detect forces along the three spatial axes with a resolution of 0.0031 N and moments with 0.0156 Nmm, was attached via an

aluminium flange. The experimental tooth on which the acting forces and moments were to be measured, a central upper incisor (11), was attached to the sensor via an adapter plate with a threaded rod. In order to investigate the force systems at a physiological oral or application temperature, the whole experimental setup including the associated Kavo Typodont model, which was attached to an aluminium profile via SAM® Axiosplit® mounting plates (SAM Präzisionstechnik GmbH, Germany), was surrounded by a thermal chamber (Fig. 1A).

By employing a temperature sensor close to the experimental tooth and a corresponding temperature controller REX-C100 PID (RKC Instrument Inc., Japan), a constant experimental temperature of 37.0 ± 0.5 °C was maintained throughout the experiment. Active self-ligating 0.022" slot straightwire brackets with MBT prescription (Bioquick, Forestadent GmbH, Germany) were placed on the Kavo Typodont model and the experimental tooth. The brackets were positioned using a passive pre-bent 0.021" × 0.025" steel wire and then fixed with a two-component epoxy adhesive.

2.2. Biomechanical measurements and simulation

Forces and moments during orthodontic tooth movement were simulated for three different scenarios: an extruded tooth, a rotated tooth, and an angulated tooth. For the simulation of the intrusion, the tooth was extruded from its idealized position in the dental arch by 1.6 mm. In the rotational movement, the starting position of the experiment corresponded to a mesial rotation of the tooth by 6°. In the final series of experiments, the starting position was defined by angulating the tooth by 10° mesially. The respective misalignments were programmed into the robot's control software, allowing them to be driven to the same starting position for all experiments. Forces and moments were determined for two 0.016" Nickel-Titanium (NiTi) leveling archwires Sentalloy Light and Sentalloy Medium (GC Corporation, Japan). Five wires of each type were examined in independent measurement cycles. The sensor's coordinate system was configured such that its x-axis corresponds to the mesiodistal axis, the y-axis corresponds to the orovestibular axis, and the z-axis corresponds to the vertical axis of the orthogonally aligned bracket slot (Fig. 1B). Consequently, a measured moment about the x-axis corresponds to a root moment, in the case of the y-axis to an angulation moment, and for the z-axis to a rotation moment. Furthermore, a positive F_z corresponds to an intrusive force, and a positive M_x corresponds to a protrusive moment.

Before engaging the archwire into the brackets, no forces or moments were acting on the test tooth or the corresponding sensor. Mathematical

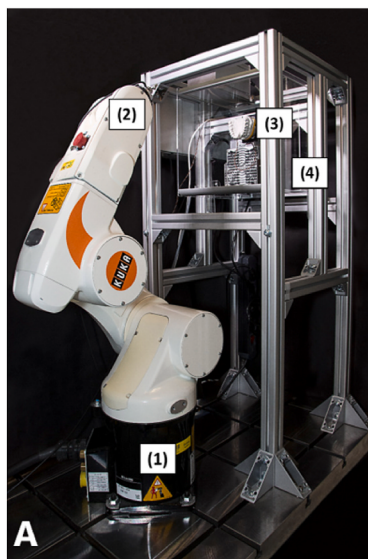


Fig. 1. A: ROSS: KUKA KR 5-sixx R650 Industrial robot (1), robot end effector with force-torque sensor and test tooth (2), KAVO Typodont model (3) within the reference frame constructed for the experiment including the thermocamber (4). B: Close-up of the experimental setup: KAVO Typodont model made of high-strength titanium alloy, force-torque sensor (indicated by a red vertical line), robot end effector and test tooth 11 with a schematic representation of the spatial coordinate system of the sensor. The direction of the measurement components along the x-(mesiodistal), y- (orovestibular), and z- (vertical) axis are shown by the arrows.

corrections within the robot program also ensured that distortions of the measurement data due to gravity or the robot's own weight or movement could be excluded. The measured force and moment values were transformed to the bracket slot or the center of force (CoF) and the center of resistance (CoR) of the tooth. This transformation was performed by geometrically measuring the distances and angles between the plane of the force/torque sensor and those of the center of force/resistance using the 3D CAD program Autodesk Inventor (Autodesk GmbH, Germany). The transformation matrix used, based on the x-y-z" convention, describes the coordinate transformations from the original coordinate system of the force/torque sensor to that of the center of force/resistance. The data was transmitted to the connected measurement computer through the robot control. After the start of the experiment, the control program calculated position corrections and the robot moved the attached tooth according to the calculated specifications, intending to cyclically reduce the forces and moments. No additional forces or moments, other than those of the archwire, were produced by the position adjustments since the robot only moved in the direction of the applied force vectors in order to reduce the forces and moments acting on it. This principle of adaptive compliance is also called force control and is an effective method that enables a robot to adapt to changing forces and moments during a task. Feedback parameters programmed into the force control determined the robot's movement sensitivity by assigning movement amplitudes to the respective force systems. The data exchange within the experiment took place until a termination condition was reached, which was defined by an asymptotic course of the forces and moments. In addition, a time limit of 10 min for communication between the robot and computer or control program was defined. The described test stand was named – "3-D Robot Orthodontic Measurement & Simulation System" (ROSS).

2.3. Statistical analysis

The Kolmogorov-Smirnov test was used to verify normal distribution, which was true for the majority of the calculated values. Therefore, the Mann-Whitney *U* test was applied as a non-parametric test for independent samples. Calculations were performed using IBM SPSS 27 (IBM Corp., Armonk, NY, USA), with a significance level of $\alpha = 5\%$.

3. Results

3.1. Intrusion

The simulated intrusion of the experimental tooth showed that, in addition to the intrusive force F_z , a protruding moment M_x around the mesio-distal x-axis occurred. The evaluation of the results showed correspondingly higher initial forces and moments for the Sentalloy

Medium archwires with $F_z = 1.637 \text{ N}$ and $M_x = 9.609 \text{ Nmm}$ compared to the Light archwire measurement series with $F_z = 1.442 \text{ N}$ and $M_x = 6.781 \text{ Nmm}$. These initial moments of the tested archwires differed significantly ($p = 0.008$). The course of the individual graphs showed that forces and moments decreased in relatively equal extent for both archwires. The scaling of the x-axis was set to a reference distance of 0.8 mm to eliminate retreats towards the end of the experiment to facilitate a comparable interpretation (Fig. 2). The realized intrusion distances only slightly differed from an average of $z = 1.089 \text{ mm}$ to $z = 1.139 \text{ mm}$ ($p = 0.690$). An intrusion over the full distance of 1.6 mm from the extruded position to the idealized physiological position was not achieved in any of the test series. The maximum intrusion was 1.346 mm (Table 1).

Additional movements in the other spatial planes occurred during the simulated intrusion. From the start of the experiment, the tooth was continuously moved mesially along the x-axis until a maximum deflection of $x = -0.101 \text{ mm}$ (Fig. 3A). In addition, there was a vestibular directed shift of the tooth along the oro-vestibular y-axis. The tooth was moved vestibularly by up to $y = 0.169 \text{ mm}$ (Sentalloy Light archwires) or within a range of $y = \pm 0.044 \text{ mm}$ (Sentalloy Medium archwires) (Fig. 3B).

3.2. Rotation

The simulated rotations showed significant differences between the Sentalloy Light and Medium archwires regarding the acting forces ($p = 0.008$) and moments ($p = 0.008$). Values of rotational moment M_z and the force in the oro-vestibular direction F_y , corresponding to a rotational movement, are presented relative to the rotation R_z of the tooth about its longitudinal z-axis for illustration (Fig. 4). Forces in the oro-vestibular direction (F_y) showed initial forces of $F_y = 0.432 \text{ N}$ (Sentalloy Medium), compared to $F_y = 0.302 \text{ N}$ (Sentalloy Light) (Table 2).

Sentalloy Light archwires showed lower initial values of $M_z = -8.271 \text{ Nmm}$ compared to the Sentalloy Medium archwires with $M_z = -9.653 \text{ Nmm}$. Additionally, the experimental tooth was derotated about 0.4° further by the Sentalloy Medium archwires compared to the simulations with the Sentalloy Light archwires ($p = 0.008$). However, a complete rotation of $R_z = 6^\circ$ was not achieved.

Additionally, movements in the mesio-distal (x) and vestibulo-oral (y) direction were observed (Fig. 5). When moving along the x-axis, the tooth was initially deflected mesially by up to $x = -0.119 \text{ mm}$ before moving distally by up to $x = 0.339 \text{ mm}$ in the further course of the experiment (Fig. 5A and B). The deflection of the tooth in the vestibular direction reached its peak with up to $y = 0.371 \text{ mm}$ after a rotation of $R_z = 1.5\text{--}2.0^\circ$. Subsequently, the tooth moved back towards the starting position but did not fully reach it by the end of the simulation, resulting in a slightly vestibular position of the tooth in all cases (Fig. 6B).

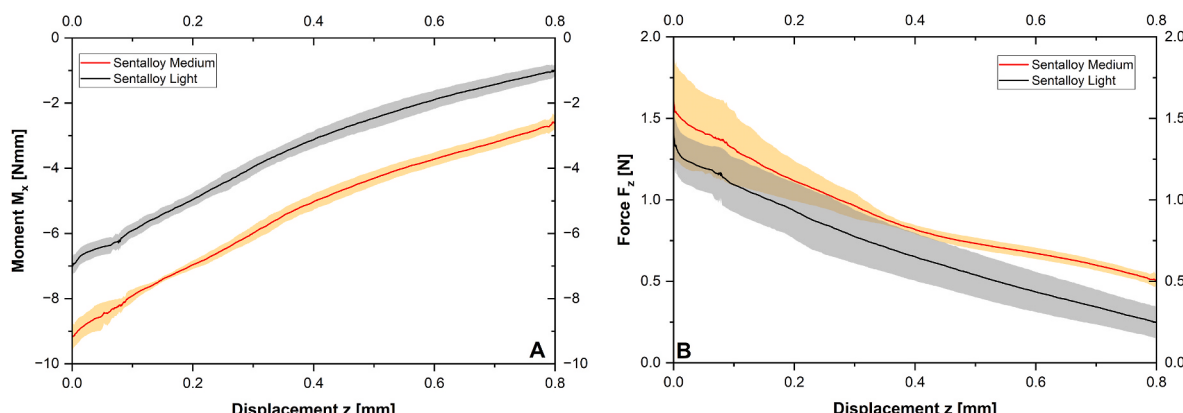


Fig. 2. A: Correlation between protrusion moment [M_x] and intrusion distance [z] B: Correlation between intrusion force [F_z] and intrusion distance [z] – Shown are the averaged curves of each archwire system with a graphically visualized standard deviation range.

Table 1

Means, maximum values (Max.), and respective standard deviations (SD) of the initial intrusion forces F_z [N], the initial protrusion moments M_x [Nm], and realized intrusion distances z [mm] for Sentalloy Light and Medium 0.016" archwires.

Archwire [Inch]	<u>F_z [N]</u>			<u>M_x [Nm]</u>			<u>z [mm]</u>		
	Mean	SD	Max.	Mean	SD	Max.	Mean	SD	Max.
Sentalloy .016 Light	1.442	± 0.127	1.545	6.781	± 0.937	8.152	1.139	± 0.173	1.346
Sentalloy .016 Medium	1.637	± 0.328	2.163	9.609	± 0.871	10.790	1.089	± 0.016	1.113
p-Value*	0.222			0.008 [†]			0.690		

*Mann-Whitney U test.

[†]Statistically significant difference.

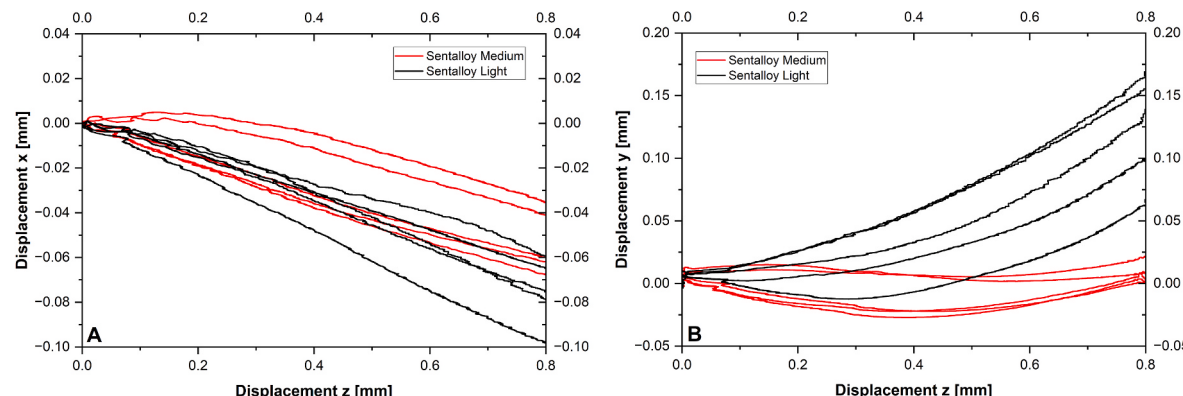


Fig. 3. A: Correlation between displacement along the mesio-distal axis [x] and the intrusion [z]. B: Correlation between displacement along the vestibulo-oral axis [y] and the intrusion [z] - Shown are the individual curves of the ten measured archwires.

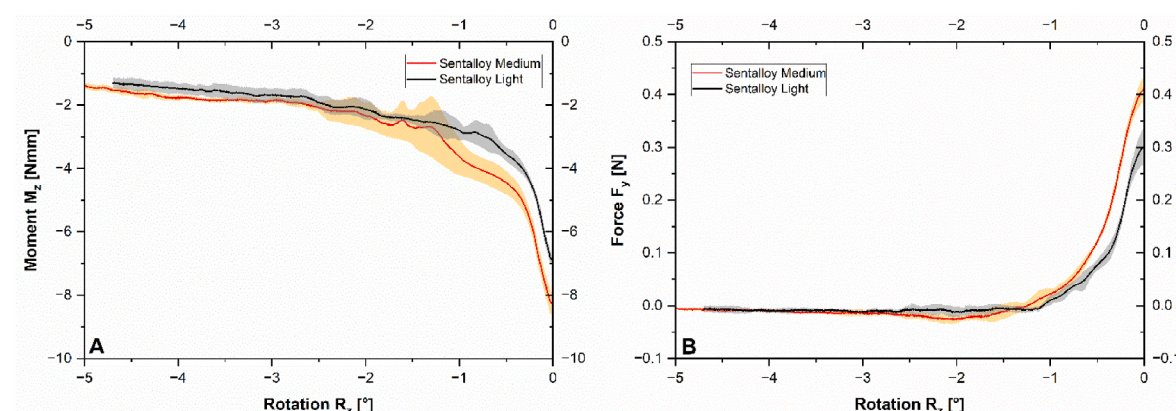


Fig. 4. A: Correlation between the de-rotational moment [M_z] and the rotation around the tooth axis [R_z]. B: Correlation between the oro-vestibular force [F_y] and the rotation around the tooth axis [R_z] - Shown are the averaged curves of each archwire system with a graphically visualized standard deviation range.

Table 2

Means, maximum values (Max.), and respective standard deviations (SD) of the initial oro-vestibular forces F_y [N], the initial rotational moments M_z [Nm] and realized rotations R_z [$^{\circ}$] for Sentalloy Light and Medium 0.016" archwires.

Archwire [Inch]	<u>F_y [N]</u>			<u>M_z [Nm]</u>			<u>R_z [$^{\circ}$]</u>		
	Mean	SD	Max.	Mean	SD	Max.	Mean	SD	Max.
Sentalloy .016 Light	0.302	± 0.036	0.349	-8.271	± 0.243	-8.477	-4.853	± 0.154	-5.056
Sentalloy .016 Medium	0.432	± 0.049	0.509	-9.653	± 0.512	-10.076	-5.316	± 0.098	-5.452
p-Value*	0.008 [†]			0.008 [†]			0.008 [†]		

*Mann-Whitney U test.

[†]Statistically significant difference.

Movements along the tooth axis (z) also occurred in two phases or directions. At the beginning of the rotation, the front tooth was intruded by up to $z = 0.122$ mm, before it extruded in the further course of the experiment (Fig. 5C). After the end of the experiment, the tooth was

therefore on average in a position extruded by $z = -0.081$ mm (Table 2).

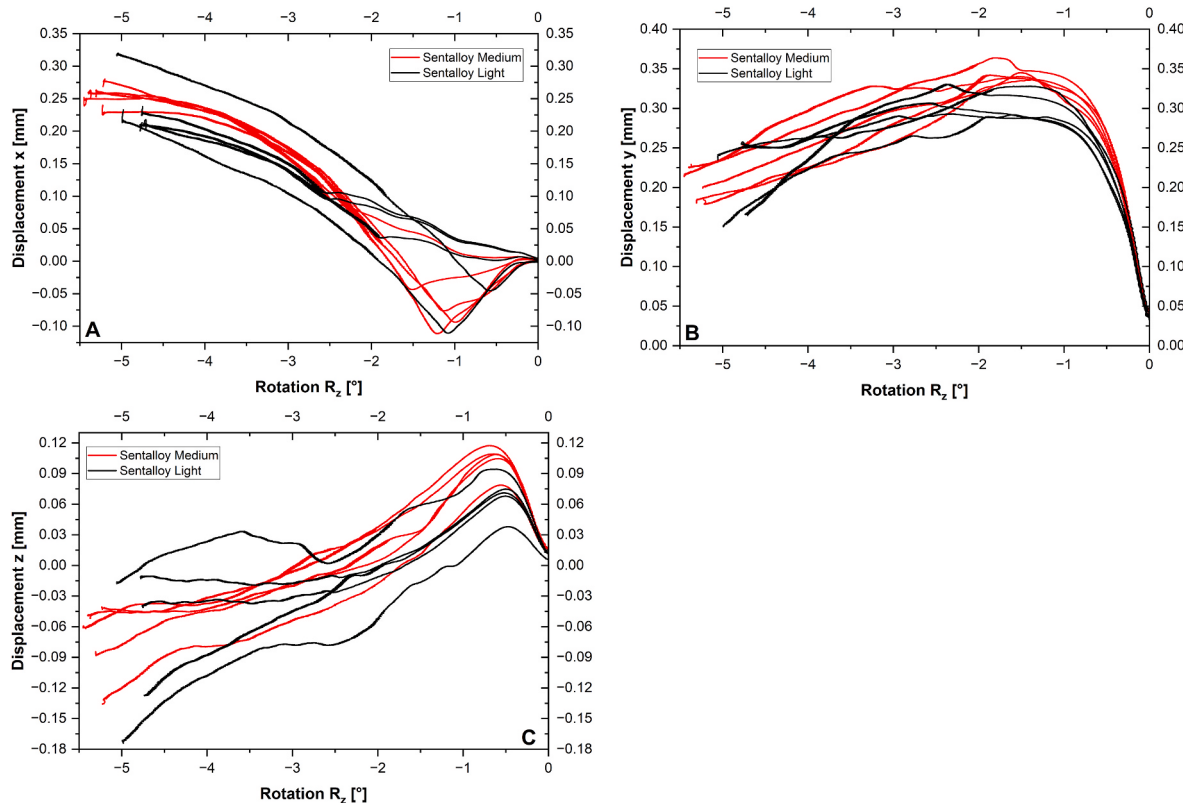


Fig. 5. A: Correlation between the displacement along the mesio-distal axis [x] and the rotation around the tooth axis [R_z]. B: Correlation between the displacement along the oro-vestibular axis [y] and the rotation around the tooth axis [R_z]. C: Correlation between the displacement along the tooth's longitudinal axis [z] and the rotation around the tooth axis [R_z]. – Shown are the individual curves of the ten measured archwires.

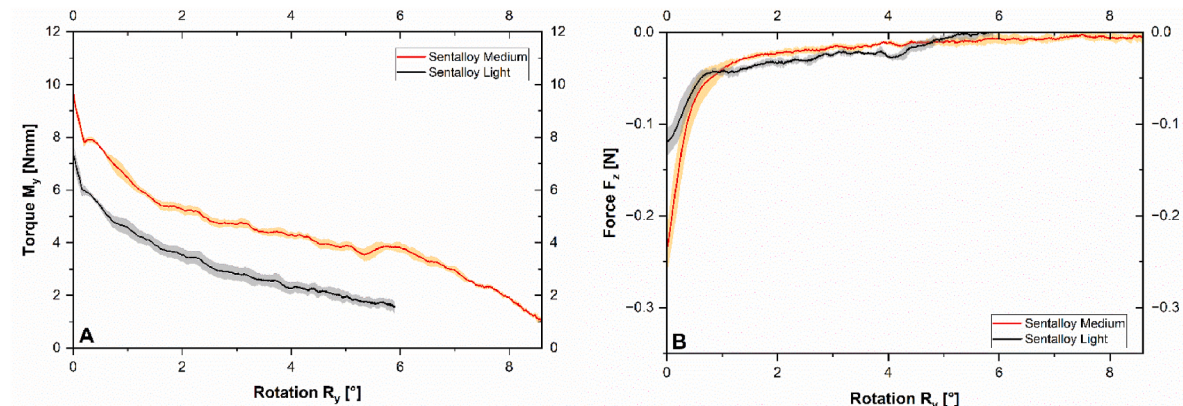


Fig. 6. A: Correlation between the up-righting moment [M_y] and the angulation or rotation around the oro-vestibular axis [R_y]. B: Correlation between the up-righting force [F_z] and the angulation or rotation around the oro-vestibular axis [R_y]. – Shown are the averaged curves of each archwire system with a graphically visualized standard deviation range.

3.3. Angulation

The simulated angulation movements showed significant differences regarding the measured forces ($p = 0.008$) and moments ($p = 0.008$) between the Light and Medium archwires respectively. The main parameters of this simulation were moments around the oro-vestibular y-axis (M_y) and the force along the tooth or z-axis (F_z), corresponding to an up-righting of the experimental tooth.

Sentalloy Medium archwires produced higher moments and forces compared to the Sentalloy Light archwires (Fig. 6). Regarding the moment around the oro-vestibular y-axis, the initial values of the Sentalloy Medium archwires, with an average of $M_y = 11.486$ Nmm, were

about 3 Nmm above the values of the Sentalloy Light archwires, with $M_y = 8.477$ Nmm. Regarding the initial force F_z , which acts in the direction of the tooth axis, the Sentalloy Medium archwires ($F_z = -0.300$ N) produced forces nearly three times as high as the Sentalloy Light archwires ($F_z = -0.122$ N). Furthermore, the Sentalloy Medium archwires were able to up-right the experimental tooth further, with an average of $R_y = 8.636^\circ$, compared to the Sentalloy Light archwires with $R_y = 6.383^\circ$. Despite a maximum root angulation of up to $R_y = 8.710^\circ$, complete up-righting of the tooth was not achieved (Table 3).

In Fig. 7 the displacements of the tooth along the three spatial axes during the simulation of the movement are represented. With approximately $x = 1.466$ mm and $x = 1.936$ mm, mainly a distally directed

Table 3

Means, maximum values (Max.), and respective standard deviations (SD) of the initial up-righting forces along the tooth axis F_z [N], the initial angulation moments M_y [Nm] and realized angulations R_y [$^\circ$] for Sentalloy Light and Medium .016" archwires.

Archwire [Inch]	<u>F_z [N]</u>			<u>M_y [Nm]</u>			<u>R_y [$^\circ$]</u>		
	Mean	SD	Max.	Mean	SD	Max.	Mean	SD	Max.
Sentalloy .016 Light	-0.122	± 0.014	-0.138	8.477	± 0.447	8.984	6.383	± 0.303	6.773
Sentalloy .016 Medium	-0.300	± 0.036	-0.331	11.486	± 0.161	11.655	8.636	± 0.045	8.710
p-Value*	0.008 [†]			0.008 [†]			0.008 [†]		

*Mann-Whitney U test.

[†]Statistically significant difference.

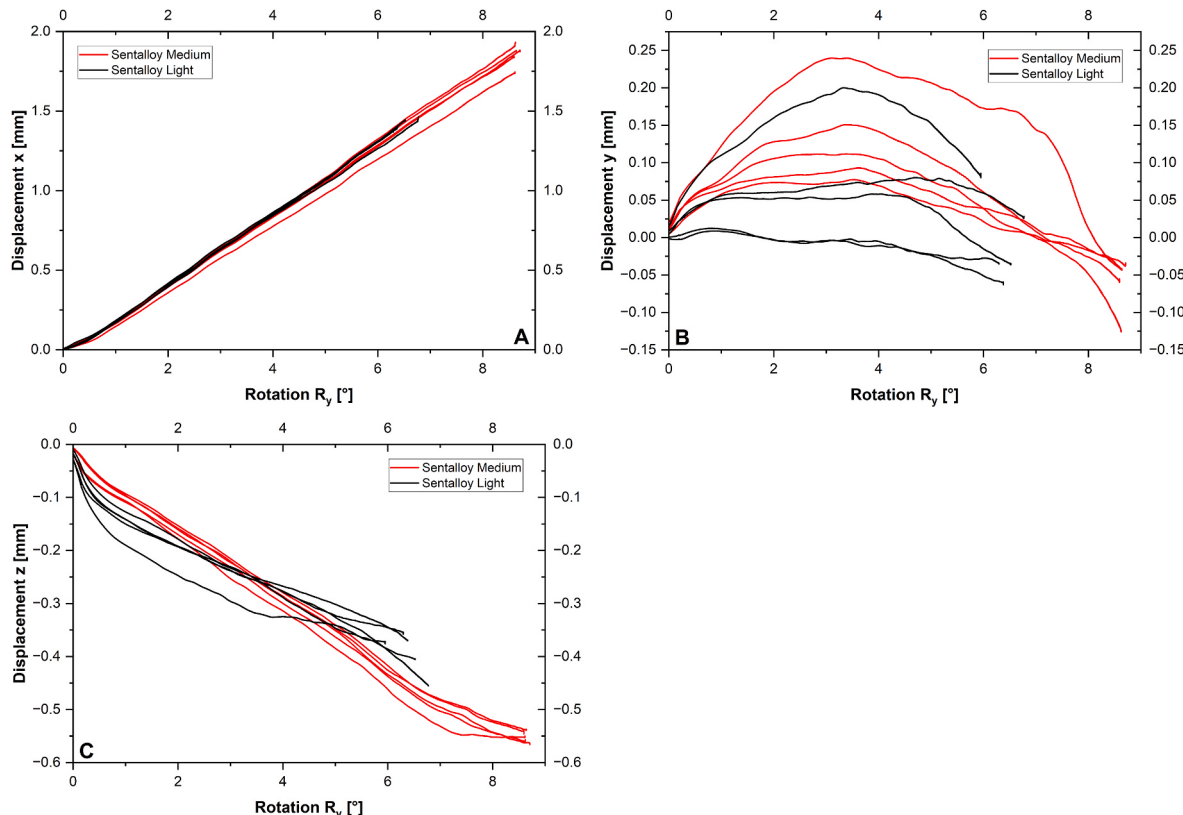


Fig. 7. A: Correlation between the displacement along the mesio-distal axis [x] and the angulation around the oro-vestibular axis [R_y] B: Correlation between the displacement along the oro-vestibular axis [y] and the angulation around the same axis [R_y] C: Correlation between the displacement along the longitudinal axis of the tooth [z] and the angulation around the oro-vestibular axis [R_y] – Shown are the individual curves of the ten measured archwires.

movement along the x-axis occurred (Fig. 7A). Additionally, the tooth was often initially deflected towards the buccal side by up to $y = 0.247$ mm after the start of the simulation before the movement direction reversed and turned back towards the point of origin. At the end of the simulation, the tooth had almost reached its starting position or slightly exceeded it (Fig. 7B). Furthermore, an extrusion movement of up to $z = -0.458$ mm or $z = -0.570$ mm along the z- or tooth-axis took place (Fig. 7C).

4. Discussion

Employing the newly developed biomechanical test stand ROSS, forces and moments were dynamically measured for three different typical scenarios of orthodontic tooth movement with a multibracket appliance during the leveling phase: rotation, angulation and intrusion.

The investigation of the force systems generated by the archwires showed that in all the experiments performed, the resulting forces and moments of the Sentalloy Medium archwires were higher than those of the Sentalloy Light. This can be explained by the fact that, due to their

material properties, the Medium archwires apply a greater force at comparable deflection than the Light versions. Furthermore, for each of the three motion simulations conducted, it was shown that the tooth did not fully return to its starting position after the completion of the trial. This is primarily attributable to the mismatch of the used archwire dimensions and the slot size of the brackets used. The angle (θ_c) by which the wire can move maximally in the slot can be calculated from the mathematical relationship between the slot width (slot), the diameter of the wire used (size), and the length of the bracket slot in mesio-distal extent (width) (Kusy and Whitley, 1999). In the conducted experiments, two round archwires with a dimension of 0.016" were used, which resulted in a maximum loss- or critical contact angle of approximately $\theta_c = 3^\circ$, taking into account the 0.022" slot width and a measured mesio-distal slot length of 0.112". In the simulated rotation and angulation movements, the physiological ideal positions were missed by 0.586–3.92°, which was close to the calculated value. In the investigated intrusion, a play of 0.006" resulted from the mismatch between the slot width (0.022") and archwires (0.016"), due to the vertical movement pattern. However, the remaining intrusion distance was

partially up to 0.021". This can be attributed to the fact that the tooth and bracket were tilted vestibularly from their neutral position due to the observed protruding moment M_x , resulting in an increased mismatch between the slot size and archwire dimension in the protruded state.

The force systems of the three different motion simulations must be evaluated separately. For rotational and angular movements with tooth misalignments of 6° and 10° as starting positions, the applied forces and moments averaged at 0.432 N and 0.3 N and 9.653 Nmm and 11.486 Nmm, which is within the physiologically acceptable range for the corresponding tooth movements (Proffit et al., 2007; Ricketts, 1976; Reitan et al., 1989). In a comparable biomechanical study, derotation movements were simulated using aligners with rotational moments of up to 71.8 Nmm, exceeding the suitable load of approximately 20 Nmm by a factor of 3.6 (Proffit et al., 2007; Hahn et al., 2010). In another study investigating thinner aligners with a thickness of only 0.3 mm, which are clinically considered inadequate due to their insufficient dimensional stability, acceptable rotational moments of 17.48 Nmm were measured, however with an intrusive force of 3.58 N as a side effect (Elkholy et al., 2017). Such high forces and moments would be expected to cause significant overloading of periodontal structures and apical root resorption (Barbagallo et al., 2008). As described in the literature, orthodontic tooth derotation with superelastic NiTi leveling archwires is more effective, biomechanically favorable and shows a lower risk of adverse effects compared to tooth derotations with aligners (Simon et al., 2014; Rossini et al., 2015; Charalampakis et al., 2018; Grünheid et al., 2017; Papadimitriou et al., 2018). Although the results of different biomechanical studies are not directly comparable, this view is supported by the results of Elkholy et al. and the results of this study in terms of the forces and moments that occur (Elkholy et al., 2017). With regard to angulation movements, no comparable biomechanical studies are available to the authors' knowledge.

In contrast to the simulation of rotation and angulation movements with suitable force and moment ranges, inadequate forces up to 1.5 N were measured for the simulated intrusion movements starting with an initial extrusion of 1.6 mm. Since the force during an axial or vertical tooth movement is only distributed over approximately 10% of the total root surface, even forces of 0.3–0.5 N may already cause increased root resorptions (Wichelhaus, 2013; Sander et al., 2011; Kurol and Owman-Moll, 1998). Consequently, the 0.016" NiTi archwires tested do not appear to be suitable for leveling a tooth extruded by 1.6 mm. One way to reduce the magnitude of the acting forces and moments while keeping the archwire dimensions constant is to use different alloys with lower force levels. However, in the case of intrusion simulation, even the Light archwires applied averaging initial forces of 1.442 N, which were significantly higher than the recommended values. Therefore, archwires with smaller diameters can be used to reduce the forces (Reddy et al., 2016; Gabersek, 2007). Reducing the archwire diameter by 0.002" was found to decrease the deflection force plateau of about 50%, and reducing the diameter by 0.004", from 0.016" to 0.012", by about 150% (Lombardo et al., 2012).

Even though the simulations with the newly developed test stand ROSS allow the investigation of the dynamic course of forces and moments of orthodontic multibracket appliances, the results of in vitro studies can only reflect the clinical situation to a limited extent (Sifakkis and Eliades, 2017). The measurements in this study refer to data transformed to the idealized center of resistance of the experimental tooth, since the forces and moments present at that point are decisive for the resulting tooth movement. Relevant clinical parameters such as the individual tooth anatomy, the dynamic shift of the center during tooth movement or the damping effect of the periodontal ligament during the initial deflection of the tooth could not be considered (Wichelhaus, 2013). Furthermore, it should be noted that the described experimental approach represents a simplification of orthodontic tooth movements, as the constant values used as feedback parameters for the robot's movement do not capture the complexity of the individual movement phases, where the velocity of tooth movement may vary (Reitan, 1957, 1960).

The archwire diameter and starting positions for the experiments were selected based on the available literature (Elkholy et al., 2017; Sander et al., 2011; Perrey et al., 2015; Jain et al., 2021; Mandall et al., 2006; Ong et al., 2011; Wang et al., 2010). However, three simplified misalignments of an experimental tooth in combination with two archwires were simulated, which does not represent the multitude of possible force systems for individual more complex malocclusions and different archwire and bracket systems.

Despite the limitations of in vitro studies, they present a valid method to investigate the behaviour of orthodontic appliances and to derive conclusions for their clinical application. The results of the present investigation show that 0.016" NiTi archwires produced forces beyond the recommended ranges for orthodontic tooth movement during simulated intrusion movements for the complete motion sequence (Wichelhaus, 2013; Ricketts, 1976; Reitan et al., 1989; Sander et al., 2011; Faltin et al., 1998). Although super-elastic 0.016" NiTi archwires have been proposed for initial leveling (Jain et al., 2021; Mandall et al., 2006; Ong et al., 2011; Wang et al., 2010), practitioners should consider using reduced archwire diameters (<0.016") when vertical deviations are present.

5. Conclusions

A novel biomechanical test stand was developed to measure the dynamic course of forces and moments during simulated orthodontic tooth movement with multibracket appliances. Within the limits of the study, 0.016" NiTi archwires generated suitable forces and moments for a derotation of 6° and an angulation of 10° of the experimental tooth, whereas forces were inadequate for a simulated intrusion of 1.6 mm.

Funding

This research did not receive any specific grant from funding agencies in the public, commercial, or not-for-profit sector.

CRediT authorship contribution statement

Benedikt Dotzer: Writing – original draft, Investigation. **Thomas Stocker:** Writing – review & editing, Methodology, Conceptualization. **Andrea Wichelhaus:** Writing – review & editing, Supervision, Project administration. **Mila Janjic Rankovic:** Writing – review & editing, Formal analysis. **Hisham Sabbagh:** Writing – original draft, Validation, Formal analysis.

Declaration of competing interest

The authors declare that they have no known competing financial interests or personal relationships that could have appeared to influence the work reported in this paper.

Data availability

Data will be made available on request.

Acknowledgements

Not applicable.

References

- Adel, S., Zaher, A., El Harouni, N., Venugopal, A., Premjani, P., Vaid, N., 2021. Robotic applications in orthodontics: changing the face of contemporary clinical care. *BioMed Res. Int.* 2021, 1–16.
- Ahuja, S., Gupta, S., Bhambr, E., Ahuja, V., Jaura, B.S., 2018. Comparison of conventional methods of simultaneous intrusion and retraction of maxillary anterior: a finite element analysis. *J. Orthod.* 45, 243–249.

- Ammar, H.H., Ngan, P., Crout, R.J., Mucino, V.H., Mukdadi, O.M., 2011. Three-dimensional modeling and finite element analysis in treatment planning for orthodontic tooth movement. *Am. J. Orthod. Dentofacial Orthop.* 139, e59–e71.
- Badawi, H.M., Toogood, R.W., Carey, J.P., Heo, G., Major, P.W., 2009. Three-dimensional orthodontic force measurements. *Am. J. Orthod. Dentofacial Orthop.* 136, 518–528.
- Barbagallo, L.J., Jones, A.S., Petocz, P., Darendeliler, M.A., 2008. Physical properties of root cementum: Part 10. Comparison of the effects of invisible removable thermoplastic appliances with light and heavy orthodontic forces on premolar cementum. A microcomputed-tomography study. *Am. J. Orthod. Dentofacial Orthop.* 133, 218–227.
- Bourauel, C., Drescher, D., Thier, M., 1992. An experimental apparatus for the simulation of three-dimensional movements in orthodontics. *J. Biomed. Eng.* 14, 371–378.
- Burstone, C.J., Koenig, H.A., 1974. Force systems from an ideal arch. *Am. J. Orthod.* 65, 270–289.
- Cervino, G., Fiorillo, L., Arzukanyan, A.V., Spagnuolo, G., Campagna, P., Cicciu, M., 2020. Application of bioengineering devices for stress evaluation in dentistry: the last 10 years FEM parametric analysis of outcomes and current trends. *Minerva Stomatol.* 69, 55–62.
- Charalampakis, O., Iliadi, A., Ueno, H., Oliver, D.R., Kim, K.B., 2018. Accuracy of clear aligners: a retrospective study of patients who needed refinement. *Am. J. Orthod. Dentofacial Orthop.* 154, 47–54.
- Chen, J., Bulucea, I., Katona, T.R., Ofner, S., 2007. Complete orthodontic load systems on teeth in a continuous full archwire: the role of triangular loop position. *Am. J. Orthod. Dentofacial Orthop.* 132, 143 e1–e8.
- Chen, J., Isikbay, S.C., Brizendine, E.J., 2010. Quantification of three-dimensional orthodontic force systems of T-loop archwires. *Angle Orthod.* 80, 566–570.
- Cicciu, M., 2020. Bioengineering methods of analysis and medical devices: a current trends and state of the art. *Materials* 13.
- de Brito, G.M., Brito, H.H.A., Marra, G.G.M., Freitas, L.R.P., Hargreaves, B.O., Magalhaes Jr., P.A.A., et al., 2019. Pure mandibular incisor intrusion: a finite element study to evaluate the segmented arch technique. *Materials* 12.
- Elkholy, F., Schmidt, F., Jager, R., Lapatki, B.G., 2017. Forces and moments applied during derotation of a maxillary central incisor with thinner aligners: an in-vitro study. *Am. J. Orthod. Dentofacial Orthop.* 151, 407–415.
- Faltin, R.M., Arana-Chavez, V.E., Faltin, K., Sander, F.G., Wichelhaus, A., 1998. Root resorptions in upper first premolars after application of continuous intrusive forces. Intra-individual study. *J. Orofac. Orthop.* 59, 208–219.
- Fansa, M., Keilig, L., Reimann, S., Jager, A., Bourauel, C., 2009. The leveling effectiveness of self-ligating and conventional brackets for complex tooth malalignments. *J. Orofac. Orthop.* 70, 285–296.
- Friedrich, D., Rosarius, N., Rau, G., Diedrich, P., 1999. Measuring system for in vivo recording of force systems in orthodontic treatment-concept and analysis of accuracy. *J. Biomech.* 32, 81–85.
- Fuck, L.M., Drescher, D., 2006. Force systems in the initial phase of orthodontic treatment – a comparison of different leveling arch wires. *J. Orofac. Orthop.* 67, 6–18.
- Gabersek, G., 2007. Kraftsysteme in Abhängigkeit von der Zahnfehlstellung: Nivellierungsbögen im Vergleich: Düsseldorf, 2007. Univ. Diss.
- Graber, L.W., Vig, K.W., Huang, G.J., Fleming, P., 2022. Orthodontics-e-book: Current Principles and Techniques. Elsevier Health Sciences.
- Grünheid, T., Loh, C., Larson, B.E., 2017. How accurate is Invisalign in nonextraction cases? Are predicted tooth positions achieved? *Angle Orthod.* 87, 809–815.
- Hahn, W., Engelke, B., Jung, K., Dathe, H., Fialka-Fricke, J., Kubein-Meesenburg, D., et al., 2010. Initial forces and moments delivered by removable thermoplastic appliances during rotation of an upper central incisor. *Angle Orthod.* 80, 239–246.
- Hayashi, K., Uechi, J., Lee, S.P., Mizoguchi, I., 2007. Three-dimensional analysis of orthodontic tooth movement based on XYZ and finite helical axis systems. *Eur. J. Orthod.* 29, 589–595.
- Jain, S., Sharma, P., Shetty, D., 2021. Comparison of two different initial archwires for tooth alignment during fixed orthodontic treatment-A randomized clinical trial. *J. Orthod. Sci.* 10, 13.
- Jeon, H.H., Teixeira, H., Tsai, A., 2021. Mechanistic insight into orthodontic tooth movement based on animal studies: a critical review. *J. Clin. Med.* 10.
- Koenig, H.A., Vanderby, R., Solonche, D.J., Burstone, C.J., 1980. Force systems from orthodontic appliances: an analytical and experimental comparison. *J. Biomech. Eng.* 102, 294–300.
- Kurok, J., Owman-Moll, P., 1998. Hyalinization and root resorption during early orthodontic tooth movement in adolescents. *Angle Orthod.* 68, 161–166.
- Kusy, R.P., Whitley, J.Q., 1999. Influence of archwire and bracket dimensions on sliding mechanics: derivations and determinations of the critical contact angles for binding. *Eur. J. Orthod.* 21, 199–208.
- Liu, Y.F., Zhang, P.Y., Zhang, Q.F., Zhang, J.X., Chen, J., 2014. Digital design and fabrication of simulation model for measuring orthodontic force. *Bio Med. Mater. Eng.* 24, 2265–2271.
- Lombardo, L., Marafioti, M., Stefanoni, F., Mollica, F., Siciliani, G., 2012. Load deflection characteristics and force level of nickel titanium initial archwires. *Angle Orthod.* 82, 507–521.
- Mandall, N., Lowe, C., Worthington, H., Sandler, J., Derwent, S., Abdi-Oskouei, M., et al., 2006. Which orthodontic archwire sequence? A randomized clinical trial. *Eur. J. Orthod.* 28, 561–566.
- Mascarenhas, R., Parveen, S., Shenoy, B.S., Kumar, G.S.S., Ramaiah, V.V., 2018. Infinite applications of finite element method. *J. Indian Orthod. Soc.* 52, 142–150.
- Ong, E., Ho, C., Miles, P., 2011. Alignment efficiency and discomfort of three orthodontic archwire sequences: a randomized clinical trial. *J. Orthod.* 38, 32–39.
- Pandis, N., Eliades, T., Bourauel, C., 2009. Comparative assessment of forces generated during simulated alignment with self-ligating and conventional brackets. *Eur. J. Orthod.* 31, 590–595.
- Papadimitriou, A., Mousoulea, S., Gkantidis, N., Kloukos, D., 2018. Clinical effectiveness of Invisalign® orthodontic treatment: a systematic review. *Prog. Orthod.* 19, 1–24.
- Perrey, W., Konermann, A., Keilig, L., Reimann, S., Jager, A., Bourauel, C., 2015. Effect of archwire qualities and bracket designs on the force systems during leveling of malaligned teeth. *J. Orofac. Orthop.* 76 (129–38), 40–42.
- Proffit, W.R., Fields Jr., H.W., Sarver, D.M., 2007. Contemporary Orthodontics, fourth ed. ed. Elsevier Health Sciences, St. Louis.
- Rajgopal, N., 2022. Finite element analysis in orthodontics. *Curr. Trends Orthodont.* 79.
- Reddy, R.K., Katar, P.K., Bypureddy, T.T., Anumolu, V.N., Kartheek, Y., Sairam, N.R., 2016. Forces in initial archwires during leveling and aligning: an in-vitro study. *J. Int. Soc. Prev. Community Dent.* 6, 410–416.
- Reitan, K., 1957. Some factors determining the evaluation of forces in orthodontics. *Am. J. Orthod.* 43, 32–45.
- Reitan, K., 1960. Tissue behavior during orthodontic tooth movement. *Am. J. Orthod.* 46, 881–900.
- Reitan, K., 1967. Clinical and histologic observations on tooth movement during and after orthodontic treatment. *Am. J. Orthod.* 53, 721–745.
- Reitan, K., 1985. Biological principles and reactions. *Orthodont. Curr. Orthodont. Concepts Techn.* 141–142.
- Reitan, K., Gruber, T., Swain, B., 1989. Biomechanische Prinzipien der Gewebsreaktion. Grundlagen und moderne Techniken der Kieferorthopädie, pp. 149–270.
- Ricketts, R.M., 1976. Biopressive therapy as an answer to orthodontic needs. Part II. *Am. J. Orthod.* 70, 359–397.
- Romanyk, D.L., Vafaeeian, B., Addison, O., Adeeb, S., 2020. The use of finite element analysis in dentistry and orthodontics: critical points for model development and interpreting results. *Semin. Orthod.* 162–173. Elsevier.
- Rossini, G., Parrini, S., Castroflorio, T., Deregbus, A., Debernardi, C.L., 2015. Efficacy of clear aligners in controlling orthodontic tooth movement: a systematic review. *Angle Orthod.* 85, 881–889.
- Sander, F.G., Ehrenfeld, M., Schwenzer, N., 2011. Zahn-Mund-Kiefer-Heilkunde Kieferorthopädie. Georg Thieme Verlag KG, Stuttgart.
- Sifakakis, I., Eliades, T., 2017. Laboratory Evaluation of Orthodontic Biomechanics: the Clinical Applications Revisited. Elsevier, *Semin. Orthod.* pp. 382–389.
- Simon, M., Keilig, L., Schwarze, J., Jung, B.A., Bourauel, C., 2014. Treatment outcome and efficacy of an aligner technique—regarding incisor torque, premolar derotation and molar distalization. *BMC Oral Health* 14, 1–7.
- Singh, J.R., Kambalyal, P., Jain, M., Khandelwal, P., 2016. Revolution in orthodontics: finite element analysis. *J. Int. Soc. Prev. Community Dent.* 6, 110–114.
- Wang, Y., Jian, F., Lai, W., Zhao, Z., Yang, Z., Liao, Z., et al., 2010. Initial arch wires for alignment of crooked teeth with fixed orthodontic braces. *Cochrane Database Syst. Rev.* CD007859.
- Wanjun, Z., Jinyuan, L., Yongping, M., Linqing, G., 2015. The development of orthodontics in the three dimensional finite element method. *J. Hebei Med. Coll. Continuing Educ.* 32, 75.
- Wichelhaus, A., 2013. Kieferorthopädie - Therapie Band 1: Farbatlanten der Zahnmédizin. Stuttgart Georg Thieme Verlag.
- Wichelhaus, A., Dulla, M., Sabbagh, H., Baumert, U., Stocker, T., 2021. Stainless steel and NiTi torque archwires and apical root resorption. *J. Orofac. Orthop.* 82, 1–12.
- Xu, H., Zhang, S., Sathe, A.A., Jin, Z., Guan, J., Sun, W., et al., 2022. CCR2(+) macrophages promote orthodontic tooth movement and alveolar bone remodeling. *Front. Immunol.* 13, 835986.
- Zhang, M., Yu, Y., He, D., Liu, D., Zhou, Y., 2022. Neural regulation of alveolar bone remodeling and periodontal ligament metabolism during orthodontic tooth movement in response to therapeutic loading. *J. World Fed. Orthod.* 11, 139–145.